



Leveraging convolutional neural networks and textural features for tropical fruit tree species classification

Can Trong Nguyen ^{a,*}, Phan Kieu Diem ^{b,**}, Dang Hieu Nghia ^c, Nguyen Kieu Diem ^b, Nguyen Thi Hong Diep ^b, Thanh-Noi Phan ^d, Vo Quang Minh ^b, Nguyen Hong Quang ^e

^a Environment Centre, Charles University, Prague 16200, Czech Republic

^b College of Environment and Natural Resources, Can Tho University, Can Tho City, Viet Nam

^c Can Tho University Software Center, Can Tho University, Can Tho City, Viet Nam

^d Department of Geography, Ludwig-Maximilians-Universität München, Munich, Germany

^e Vietnam National Space Center (VNCS), Vietnam Academy of Science and Technology (VAST), 18 Hoang Quoc Viet, Hanoi 100000, Viet Nam

ARTICLE INFO

Keywords:

Tropical fruit trees
Conventional neural network (CNN)
Machine learning models
Spectral bands
Textural features
Artificial intelligence

ABSTRACT

Mapping fruit tree species is an essential task in agricultural planning and management. However, the classification of tropical fruit tree species faces many technical challenges because of their identical leaf characteristics, especially in developing countries with limited accessibility to data and advanced technologies. This study attempts to evaluate the effectiveness of currently available satellite images (Sentinel-2 and Planet) and Gray-level co-occurrence matrix (GLCM) textural features in discriminating tropical fruit trees using a conventional neural network (CNN) compared to other machine learning algorithms. Spectral bands and textural features from Sentinel-2 and Planet images were extracted to input into the CNN model, as well as other five commonly used machine learning models, including K-Nearest Neighbor (KNN), Gradient Boosting Machine (GBM), Naive Bayes (NB), Random Forest (RF), and Support Vector Machine (SVM). The classification results were evaluated based on performance metrics of accuracy, F1-score, and spatial agreement of classified maps. The contribution of each variable in the classification was identified using permutation feature importance. The research findings revealed that the CNN model outperformed the other machine learning models in detecting five major fruit trees (i.e., coconut, coconut intercropping, durian, pomelo, and rambutan). The most important contributions to mapping performance were constituted by spectral bands from Sentinel-2 (e.g., shortwave infrared-SWIR, Blue, and Vegetation Red-Edge bands), while Planet image provides vital textural information such as Entropy (ENT), Angular Second Moment (ASM), sum average (SA), and homogeneity (HOM). The research provides valuable insights into classifying tropical fruit trees using entirely free data sources, avoiding the need for costly and complex alternatives. It also presents significant potential for applications in other tropical regions, contributing to sustainable agricultural management.

* Corresponding author.

** Corresponding author.

E-mail addresses: can.nguyen@czp.cuni.cz (C.T. Nguyen), pkdiem@ctu.edu.vn (P.K. Diem).

1. Introduction

Fruits are an essential component of a healthy diet, as they are rich in fiber, vitamins, minerals, electrolytes, and antioxidants, thereby assisting in control of chronic diseases and body weight management (Pem and Jeewon, 2015; Slavin and Lloyd Beate, 2012). Fruit trees (or orchards) are a typical ecosystem that can generate both ecological and economic benefits for indigenous communities, supporting environmental protection against desertification and alleviating poverty (Xia et al., 2020). It is obvious that fruit trees provide huge provisioning services (food, fiber, and nutrients) and increase farmers' income. For example, in Vietnam, the income from fruit cultivation is 2–3 times higher than that from rice cultivation (Thuong and Ha, 2013). As a type of plantations, they also participate in generating various supporting and regulating services, such as soil retention, water conservation, carbon sequestration, climate regulation, habitat provision, and aesthetic and cultural values (Wang et al., 2023). In some areas, farmers often spontaneously convert from agricultural land to fruit trees and from one type of fruit tree to another due to market demand and high profits (Hanh et al., 2017). This trend can disrupt the planning of specialty fruit-growing areas and complicate effective management of pests and diseases. Therefore, there is a need for robust and accurate mapping of fruit-growing areas to support growth monitoring, prevention of diseases and insect pests, yield and productivity estimation (Zhou et al., 2022a).

Fruit species can be primarily grouped into three categories based on their geographic and distributed climate, including tropical fruits (jackfruit, durian, rambutan), subtropical fruits (lychee, avocado, kiwi), and temperate fruits (apple, pear, peach, plum) (Ozdarici Ok and Ok, 2023a). It differs from subtropical and temperate fruit species. Tropical fruit trees are complicated to identify using remote sensing data because they are often grown in highly dense and multilayer canopies with relatively similar spectral signatures (Pereira Martins-Neto et al., 2023; Sothe et al., 2019). Moreover, tropical species have less pronounced seasonal changes compared to temperate species. Their leaf phonologies are identical, limiting the effectiveness of seasonal remote sensing data for identifying and distinguishing species.

Local authorities usually adopt traditional manual surveys to estimate and draw regional fruit-growing maps. However, this method has many problems, such as the time, cost, and labor required for long-term surveys or subjective differences in surveyors' criteria that can lead to inconsistent results (Zhou et al., 2022a). Developing state-of-the-art remote sensing data sources and analysis techniques effectively encourages many applications in agriculture and fruit tree species mapping (Ozdarici Ok and Ok, 2023a). There are three major approaches to discriminating fruit/tree species, including (1) hyperspectral data sources (Deng et al., 2020; Ferreira et al., 2016; Upadhyay et al., 2019), multitemporal analysis (Peña et al., 2017; Zhou et al., 2022a), and very high-resolution images from Unmanned Aerial Vehicle (UAV) (Dong et al., 2020; Tian et al., 2022). The first approach exploits the differences in spectral signatures between species within a narrow spectral range to distinguish tree species. The multitemporal time series are applied on Landsat, Sentinel-2, and even active SAR (Synthetic Aperture Radar) to capture seasonal variations between species because of leaf phenology across seasons. As mentioned, it is deemed more suitable for temperate fruit species than tropical species without significant plant phenology changes. Moreover, obtaining a continuous optical time series is substantially challenging for tropical monsoon regions. The third approach accounts for a large proportion of methods used for fruit tree detection regardless of climate region (Ozdarici Ok and Ok, 2023a). Very high-resolution images from UAVs can even carry hyperspectral sensors, assisted by object recognition and object-based image analysis (OBIA), which can achieve accurate species detection. Yet, it is frequently utilized to monitor smallholder farms because it is challenging to collect and process data for an extensive area using UAVs. Although these methods have high performance, approaching hyperspectral and very high-resolution images is strenuous, especially in developing countries over a large area.

In addition to spectral and temporal changes, textural features also considerably contribute to the accuracy of land use, land cover classification using remote sensing data. They have been effectively applied in land use, land cover classification (Iqbal et al., 2021; Kabir et al., 2010; Kupidura, 2019). For example, vegetation types and rubber plantations were successfully identified by combining Sentinel-2 spectral bands and textural indices (Mohammadpour et al., 2022; Zhang et al., 2020). They not only represent the surface brightness/gray tones but also reflect the spatial distribution and structural information of surface objects (Zhang et al., 2020). Spectral signatures are the result of interactions between solar radiation and surface materials or chlorophyll in leaves and are therefore highly dependent on weather, environment, and plant conditions (Nguyen et al., 2023). In contrast, textural features are relatively stable and can characterize canopy features. Distinguishing tropical fruit species using textural features has promising potential.

Convolutional Neural Networks (CNNs) have proven to be highly effective in image processing, particularly in crop classification and object recognition. Unlike traditional machine learning models, CNNs automatically extract features from raw data without the need for manual techniques, which saves time and reduces reliance on user expertise (Yang and Xu, 2021; Liu et al., 2017). By utilizing convolutional and pooling layers, CNNs maintain the spatial relationships between pixels, enabling them to detect features like edges, textures, and shapes (Yang and Xu, 2021; Liu et al., 2017). Additionally, due to their multilayer structure, CNNs learn hierarchical features that range from basic elements such as edges and corners to more complex structures like shapes and objects (Yang and Xu, 2021). This capability allows CNNs to recognize intricate patterns more effectively than traditional machine learning models (Liu et al., 2017). Numerous studies have highlighted the superior performance of CNNs. For instance, a 13-layer CNN achieved an accuracy of 94.94 %, which is at least 5 % higher than other methods (Liu et al., 2017). Another study focused on classifying fruits by family using CNNs, achieving an accuracy of 99.82 %, thereby outperforming both ResNet-20 and SVM (Kumar et al., 2022). Additionally, CNNs support transfer learning, which enhances their utility on smaller datasets (Yang and Xu, 2021). The application of CNNs for classifying fruit trees, particularly in tropical regions, holds significant promise for agricultural research and modernizing farming practices (Rahaman et al., 2018; Mureşan and Oltean, 2021).

In the current context of increasing diverse remote sensing data sources with relatively good spatial and spectral resolution data being increasingly opened for public access, such as Seninel-2 (13 spectral bands, 10 m) and Planet NICFI (approximate 5 m, Norway's

International Climate and Forest Initiative). This study ambitiously establishes a methodological framework to identify tropical fruit species based on a combination of available medium-high resolution images and textural features that can be subsequently established as a basis for large-scale mapping. More specifically, it evaluates the classification performance of a deep learning model compared to other commonly used machine learning models from disparate perspectives. The research findings of this study have important methodological implications for replication and further development for similar areas in tropical climates, where classification of tropical fruit species is often a demanding task.

2. Materials and methods

2.1. Study area

Ben Tre is one of the top three leading provinces in the Vietnamese Mekong Delta in terms of orchard area. This is also a principal economic region planned to develop 12 main types of tropical fruits. Some typical fruits in Ben Tre that are famous for their quantity and quality include rambutan (*Nephelium lappaceum*), durian (*Durio zibethinus* L.), mangosteen (*Garcinia mangostana*), star apple (*Chrysophyllum cainito*), pomelo (*Citrus Maxima*), longan (*Dimocarpus longan*), and langsat (*Lansium domesticum*). This is also home to the most immense coconut farms in Vietnam, with an area of approximately 78,000 ha (2023). In 2020, the total orchard area is approximately 26,641 ha, which provides about 300 thousand tons of fruits per year, mainly distributed in Cho Lach and Chau Thanh districts (about 30 % of each district).

Regarding geographic location, Chau Thanh is located North of Ben Tre province, which has an area of 22,500 ha (Fig. 1). It is likely an island separated by intricate rivers and canals. Chau Thanh possesses favorable natural conditions for developing agriculture and fruit cultivation. More specifically, the terrain is relatively flat (~3 m above sea level) (Thu et al., 2013). It is dominated by the tropical monsoon climate with stable and high average temperatures (26–27 °C) and high precipitation (Ba and Nhung, 2013). Furthermore, the district is located between the tributaries of the Mekong River, My Tho and Ham Luong rivers, with fertile alluvial soil and abundant freshwater. Although saltwater intrusion in the dry season is observed yearly, it is frequently mild during a short period. Local communities also have a long terms experience cultivating and breeding fruit trees for about 40 years. Therefore, these favorable conditions allow Chau Thanh to become one of the vital fruit production districts of the province. The main fruit tree area in Chau Thanh District primarily consists of coconut, durian, pomelo, and rambutan, which together account for 70.7 % of the district's total land area. This cultivation plays a vital role in the livelihoods of local residents. In response to the current issue of scattered farming practices, the district's agricultural sector is being restructured into concentrated growing areas that promote sustainable development. Therefore, applying technology to manage these growing spaces is crucial for district administrators.

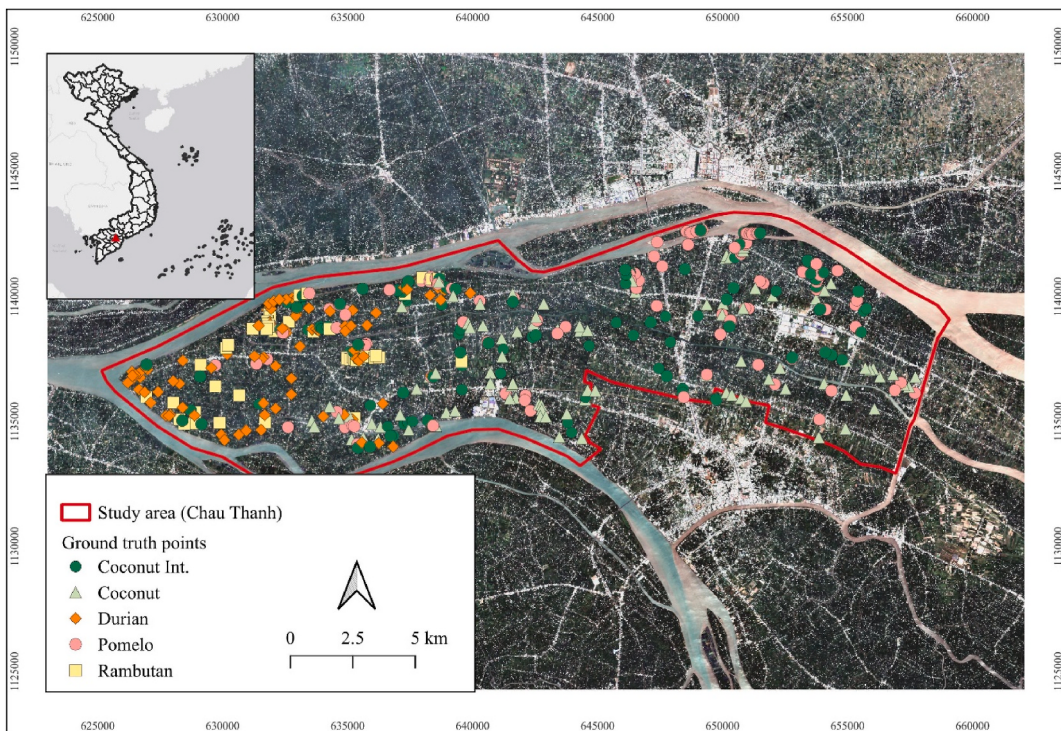


Fig. 1. Chau Thanh district in Southern Vietnam and locations of ground truth points collected during field survey campaigns. The background is Sentinel-2 image (True color composite).

2.2. Satellite images and preprocessing procedures

This study adopts and combines two optical satellite images as the primary data sources for fruit tree classification. The first data source is Sentinel-2 Level 2A, a medium-to-high-resolution optical satellite imagery product that is widely regarded as one of the best freely available datasets for recent land monitoring (Phiri et al., 2020). Its multispectral imager (MSI) sensor can provide a wide range of spectral bands from visible and near-infrared to shortwave infrared spectrum (Table 1). Additionally, the spatial resolution is relatively high, up to 10 m at its highest. Therefore, it is essentially useful for detecting and distinguishing many land use and land cover features, even those that are small in size and have similar spectral reflectance—challenges that are difficult to overcome with previous satellite imagery (Phiri et al., 2020; Segarra et al., 2020). Moreover, the Level 2A data provides bottom-of-the-atmosphere (BOA) reflectance, enhancing information while limiting atmospheric effects in the tropics (Vrdoljak and Kilić Pamuković, 2022). This makes the classification in this tropical region more efficient. The fruit trees in the research area are evergreen and do not exhibit significant seasonal variations in leaf phenology as in temperate regions. Therefore, instead of collecting multi-temporal images, which are likely to be heavily affected by clouds due to the tropical coastal region, the study acquired quality scenes with the lowest cloud coverage. We acquired one cloud-free scene of Sentinel-2 (L2A) from Copernicus Data Space Ecosystem (<https://dataspace.copernicus.eu/>). This image was captured on February 25, 2020 (10:17 a.m. local time) with a cloud cover rate of 0.993 % for the classification. We directly utilized four visible and near-infrared (NIR) bands at 10-m resolution. Although the other six medium-resolution bands (i.e., four vegetation red edge bands and two shortwave infrared bands) have coarser spatial resolution at 20 m, they can provide valuable spectral information to capture and distinguish diverse leaf characteristics among fruit trees based on a wider spectral range given by these six bands. To match the high-resolution bands, these bands were resampled to a pixel size of 10 m using the nearest resampling method. The preprocessing procedures, including resampling, layer stacking, and cropping of the study area bounded image, were performed using terra (Spatial Data Analysis) package in R-4.4.2.

This study also leverages the Planet (Planet-NICFI) surface reflectance basemap distributed through Google Earth Engine (GEE) platform. This freely available high-resolution data (~5 m) is expected to enhance fruit tree discrimination by better spatial resolution that might be missed on Sentinel-2 images. The Planet-NICFI basemap is a mosaic data collection combining PlanetScope and RapidEye images for the initial purpose of forest tracks (Pandey et al., 2023; Zhang et al., 2023). Image scenes are processed by a procedure of scene selection, atmospheric correction, cloud mask, and normalization to produce monthly cloud-free images (Dalagnol et al., 2023). We collected cloud-free images from the Tropical Asia data collection in June 2020 to match the Sentinel-2 data above. The pre-processing steps, including applying date and location filters, generating a median composite image, and clipping to the study area, were conducted using algorithms in GEE. The preprocessed output with four spectral bands (Table 1) at ~5-m resolution was then exported from GEE for further processing steps outside of the platform.

2.3. Reference data

Ground truth point collection is a vital dataset in satellite image classification as it plays a key role in both training and validating the classifier. We collected the ground truth points in the study area through field data collection campaigns in April 2020. Field survey groups were allocated different routes, mainly along major roads to facilitate movement and cover the entire study area. Each group was equipped with a handheld GPS or a mobile GPS application of *Mapinr* to mark the location of the corresponding land cover types and fruit tree parcels. The parcel is selected that should be large enough to ensure its representativeness and identification on images. We also made an effort to reach the center of the parcel to mark its location, aiming to minimize possible errors caused by equipment. A total of 690 ground truth points were collected through the field survey campaigns, which record diverse land cover categories and main fruit tree species such as coconut (156), coconut intercropping (coconut Int., 127), pomelo (170), durian (155), and rambutan

Table 1
Spectral bands and resolution of acquired satellite products.

Satellite/Product	Bands/Functions	Central wavelength (nm)	Resolution (m)
Sentinel-2 MSI (L2A)	B1 – Ultra blue (coastal aerosol)	443	60
	B2 – Blue	490	10
	B3 – Green	560	10
	B4 – Red	665	10
	B5 – Vegetation Red Edge 1	705	20
	B6 – Vegetation Red Edge 2	740	20
	B7 – Vegetation Red Edge 3	783	20
	B8 – Near Infrared	842	10
	B8A – Vegetation Red Edge (narrow)	865	20
	B9 – Water vapor	940	60
	B10 – Cirrus	1,375	60
	B11 – Shortwave Infrared (SWIR1)	1,610	20
	B12 – Shortwave Infrared (SWIR2)	2,190	20
Planet-NICFI	Band 1 – Blue	480	4.77
	Band 2 – Green	540	4.77
	Band 3 – Red	630	4.77
	Band 4 – Near Infrared (NIR)	830	4.77

(82) (Figs. 1 and 2).

However, these samples are supposed to be insufficient for a deep-learning model to distinguish fruit tree species. The more the sample points, the more accurate the model. Therefore, we expanded the training dataset mainly based on these ground truth points and other auxiliary data using QGIS 3.30.3 and digitization tools. We only expanded the marked point into a polygon by including its neighboring pixels with uniform characteristics instead of drawing unintentionally. Ultimately, 147,236 pixels were collected for training and testing the model.

2.4. Textural features

Gray-level co-occurrence matrix (GLCM) texture is a widely used method to extract textural features in high-image analysis (Park and Guldmann, 2020). GLCM stands on statistical methods to characterize the spatial relationships between pixels in an image (Alzhanov and Nugumanova, 2024). It considers the distribution of gray levels across adjacent pixels to estimate the frequency of similar-intensity pixels against different-intensity pixels based on two parameters of distance and direction (Mohammadpour et al., 2022). This study adopted nine indices to extract spatial and textural features on Sentinel-2 and Planet images (Table 2) (Hall-Beyer, 2017; Park et al., 2016).

These indices are estimated based on gray-level consideration, while each satellite image has multispectral bands. Different bands reflect unique information about features, which is fairly important in image analysis. Therefore, we used principal component

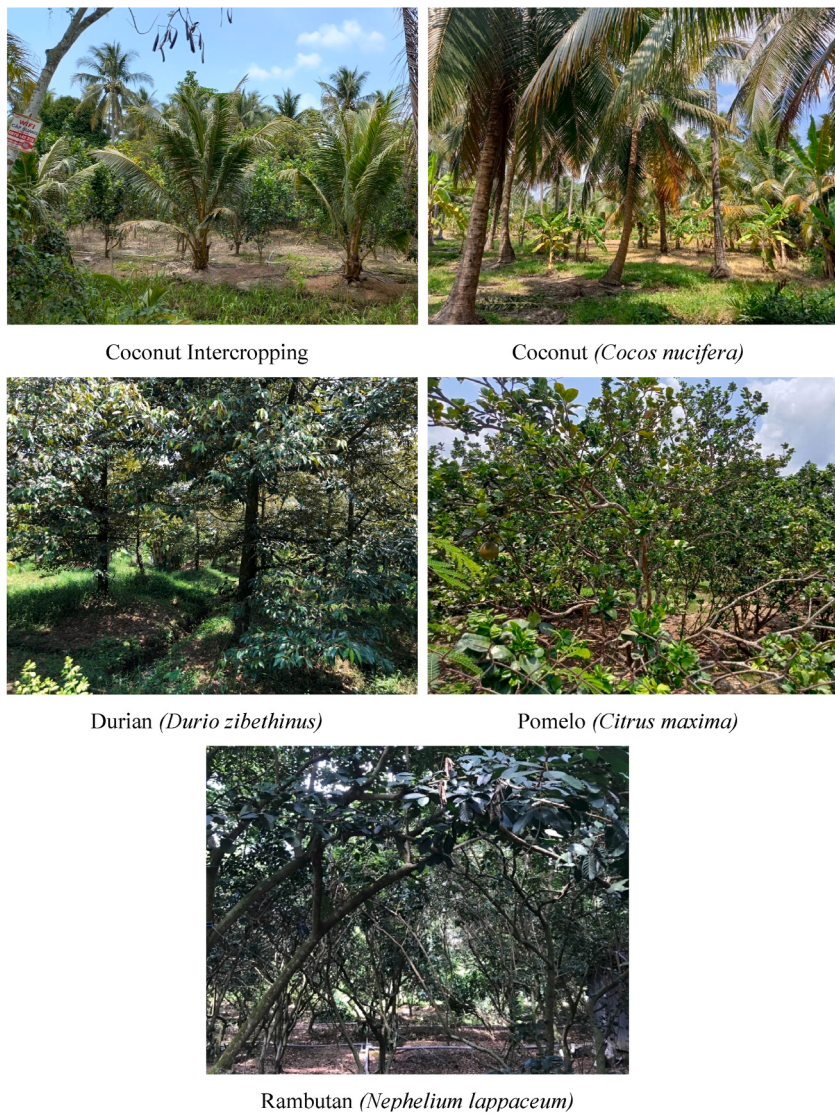


Fig. 2. Field photos of five major fruit tree species demonstrate potential differences in distribution and canopy structure. Source: Authors own field photos.

analysis (PCA) to synthesize spectral information from all bands into the first component (grayscale) for the GLCM analysis (Mohammadpour et al., 2022). The dimension reduction of PCA was completed using RStoolbox in R-4.4.2. According to an empirical study reported by Zhang et al. (2020), an optimum moving window of 15×15 was applied to calculate the GLCM texture indices for the Sentinel-2 image. With a resolution twice as fine as Sentinel-2, the GLCM textural features of Planet were estimated using a moving window of 31×31 . The GLCM textural indices were calculated based on GLCMTTextures package in R-4.4.2.

2.5. Data normalization and information extraction

Sentinel-2 and Planet images are encoded in different data levels (bit depth). Textural value ranges are also disparate between indices. It is challenging for machine learning models, which work better with scaled data than original digital numbers. Each information band was then normalized to spread the image values between 0 and 1 according to Equation (1).

$$xscaled = \frac{x - xmin}{xmax - xmin} \quad (1)$$

Subsequently, we extracted values of normalized bands at reference polygons. This dataset was randomly split into two isolated datasets: training (70 %, 103,067 pixels) and validation (30 %, 44,169 pixels) datasets (Can et al., 2021).

2.6. Convolutional Neural Network

Convolutional neural network (CNN) is a deep learning model expected to boost model convergence and improve classification performance compared to traditional classifiers. We used 1D-CNN model to analyze input features (i.e., spectral bands and textural features) as one dimension data using the concepts of pixel-based classification. The 1D-CNN model was selected to leverage the model's simplicity compared to 2D-CNN and 3D-CNN, while it emphasizes how spectral and textural information contribute to the classification of fruit tree species. The training data is location-based and collected using GPS device, which is inherently better represented by a one-dimensional vector of spectral band and textural features rather than 2D spatial image. Moreover, the machine learning models used for comparison are also one-dimensional, so employing the 1D-CNN ensures a fair peer-to-peer comparison and minimizes biased evaluation between models.

This study built a relatively light CNN model with fewer hidden layers and parameters using the Keras Sequential (Fig. 3). The model begins with combining two Conv1D layers to filter the input data and allow the network to learn more complex features. These layers use the same number of neurons ($n=128$) and a kernel size of 2. A parameter of padding (*Same*) was introduced to ensure the output from filter has the same length as the input by padding the edges. Subsequently, a 1D max polling was added to reduce the output length by half and retain the most prominent features by taking maximum values. This consideration moves over a window size of 2. The first layer ends up with a “Dropout” function to prevent overfitting, which randomly sets a fraction of input units to zero (20 %).

The second conventional block has relatively similar parameters to the first block. However, it has a double filter ($n=256$). In both conventional blocks, the activation function was ReLU (Rectified Linear Unit) (Eq. (2)), which introduces non-linearity to approximate complex functions and learns intricate patterns from data.

$$ReLU(x) = \max(0, x) \begin{cases} x > 0, x = x \\ x \leq 0, x = 0 \end{cases} \quad (2)$$

Table 2

Textural features and corresponding equations.

Textural features	Equation	Description
Angular Second Moment (ASM)	$\sum_{i,j=0}^{N-1} P_{i,j}^2$	ASM represents the image's roughness, which is rougher with a higher ASM value.
Contrast (CON)	$\sum_{i,j=0}^{N-1} P_{i,j}(i-j)^2$	CON is also called a sum of squares variance. It reveals the textural thickness. The higher value of CON describes the more different between adjacent pixels.
Correlation (COR)	$\sum_{i,j=0}^{N-1} \left[\frac{(i - \mu_i)(j - \mu_j)}{\sqrt{\sigma_i^2 \sigma_j^2}} \right]$	COR measures the linear dependency of gray levels on neighboring pixels in rows and columns. A higher correlation has a greater value of COR.
Dissimilarity (DIS)	$\sum_{i,j=0}^{N-1} P_{i,j} i - j $	DIS reflects another aspect of image's heterogeneity.
Entropy (ENT)	$\sum_{i,j=0}^{N-1} P_{i,j}(-\ln P_{i,j})$	ENT gives rich information within a window. The more complex the texture inside a considering window, the higher the value of ENT.
Homogeneity (HOM)	$\sum_{i,j=0}^{N-1} i \frac{P_{i,j}}{1 + (i - j)^2}$	HOM characterizes the smoothness of the image. A smoother and more uniform image has a higher value of HOM.
Mean (MEA)	$\sum_{i,j=0}^{N-1} i(P_{i,j})$	MEA reflects the average value or brightness in the moving window.
Variance (VAR)	$\frac{\sum_{i,j=0}^{N-1} (P_{i,j} - \mu)^2}{N - 1}$	VAR highlights the contour of each homogenous polygon in terms of gray level.
Sum average (SA)	$\sum_{i=0}^{N-1} iP_{x+y}(i)$	SA measures mean values of the sum of pixel intensities in images derived from gray levels.

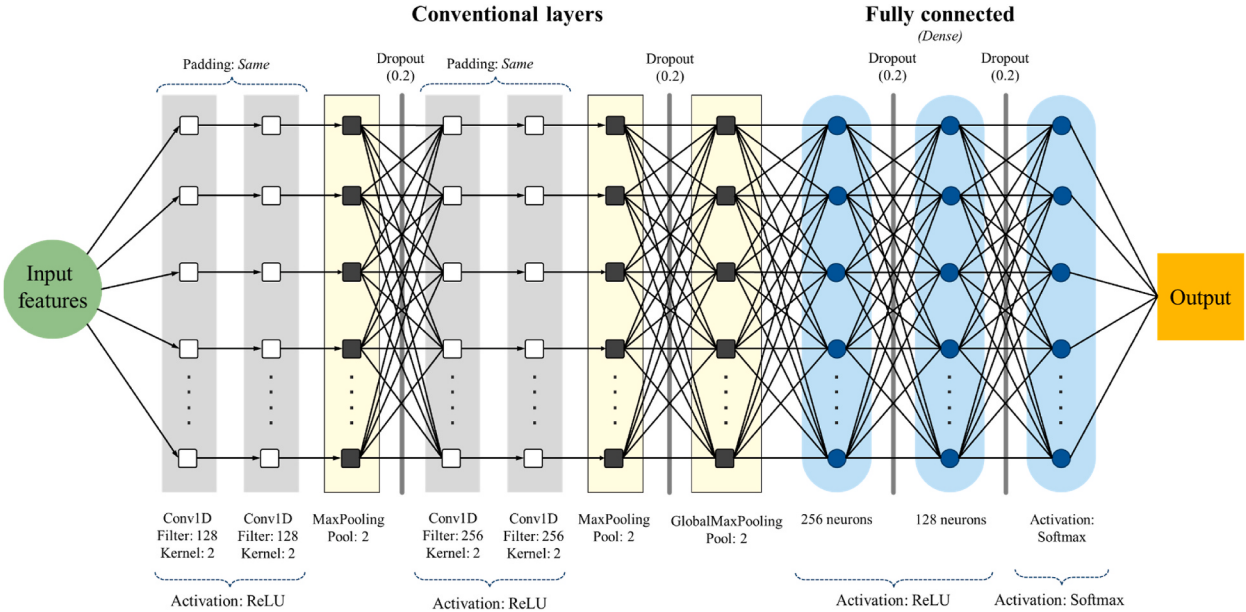


Fig. 3. The proposed concept of CNN model architecture.

A global max polling one-dimensional layer reduces the dimensionality of output from conventional layers to a single layer. It takes maximum values over the time dimension for each feature map, thereby summarizing the presence of features over the entire input sequence.

Fully connected layers consist of two dense layers using the activation function of ReLU to learn high-level features. The first dense layer has 256 neurons, and the second dense layer reduces half the number of neurons (128). After each dense layer, the dropout function (20 %) was introduced to restrain the overfitting. The final output layer was obtained by applying Softmax activation function (Eq. (3)), which converts the raw output scores from the network into probability distribution over multiple classes in the classification task.

$$\sigma(z_i) = \frac{e^{z_i}}{\sum_{j=1}^n e^{z_j}} \quad (3)$$

The CNN model was then examined by an optimizer of Adam (Adaptive Moment Estimation) to improve the training accuracy and minimize the loss function, thereby enhancing the model's performance. Adam is widely adopted in land use, cover classification tasks, which takes advantage of two other optimizers (i.e., AdaGrad and RMSProp) (Eq. (4))—AdaGrad works well for sparse gradients and RMSProp is good for non-stationary settings (Bhosle and Musande, 2019). Adam is effective when working with large datasets and parameters without much memory and resources. A categorial cross-entropy loss function was combined with Softmax activation function for a multi-classes classification (Sameen et al., 2018).

$$m_t = \beta_1 m_{t-1} + (1 - \beta_1) g_t \quad (4)$$

2.7. Machine learning models

In addition to CNN, this study also examined the classification performance of five other machine learning models, commonly applied in land use and land cover classification using satellite images. K-Nearest Neighbor (KNN) is a non-parametric supervised algorithm without demands on class density function. It assigns a class to a data point that is the most identical to the sample on the training data based on Euclidean distance basis and given initial k value (Prasad et al., 2022). Gradient Boosting Machine (GBM) is a widely used algorithm in LULC classification using satellite images. It takes advantage of ensemble machine learning algorithms by employing decision trees in its classifiers (Nery et al., 2016). Although GBM has been efficiently applied in several applications, even in species prediction, its application in recent studies is overshadowed by state-of-the-art machine learning classifiers because it may lead to overestimation and having many parameters to tune (Georganos et al., 2018). Naive Bayes classifier (NB) stands on the Bayes theorem to estimate the probability of chance for an event. It uses strong/naive assumptions of independence between features to calculate the probability of a data point belonging to a land use class rather than another based on feature values and classify each data point in the dataset (Palanisamy et al., 2023). Random Forest (RF) is among the most applied machine learning classifiers for LULC classification tasks. RF has the advantages of a non-parametric algorithm, high classification accuracy, and robustness to noises with fewer parameters to be set against other classifiers (Pal, 2005; Tikuye et al., 2023). It consists of many decision tree models trained by

bootstrap sampling, which considers some vectors more than once in a classifier thereby improving the classification accuracy. In the RF model, the number of trees (ntree) parameter should be large enough to ensure that every data point is considered at least once. The final model is Support Vector Machine (SVM), which uses an optimally separating hyperplane to classify categories. It is especially appropriate for high-dimensional datasets with less training sample requirements than other algorithms (Nguyen et al., 2022; Noi and Kappas, 2018). In land use and land cover classification tasks, the common kernel used in SVM is the radial basis function (RBF) kernel (Jodzani et al., 2019). These machine learning models were initialized and trained using scikit-learn, which is the most popular open-source machine learning library in Python. This library also gives us different tools for model selection, validation, and tuning model parameters. The hyper-parameters of the above machine-learning models were tuned using grid search function (GridSearchCV) to detect the optimum parameters for each model (Table 3).

2.8. Performance assessment

The classification tasks were evaluated by a confusion matrix based on the true labels and predicted labels. Four variables were then extracted, which include true positive (TP), true negative (TN), false positive (FP) and false negative (FN). Specifically, TP occurs when the model correctly predicts a positive class. TN is an outcome when the model correctly predicts a negative class. FP appears in case the model incorrectly predicts a positive class (Type I error). FN is an outcome of a false prediction for a negative class (Type II error). These are vital variables to estimate accuracy parameters of accuracy, precision, recall, and F1-score to evaluate the performance and correctness. Accuracy measures the overall power of the model's prediction. Precision measures the accuracy of the positive prediction. A higher precision value indicates that the model returns more relevant labels than irrelevant labels. Recall reflects the model's ability to catch all relevant labels. F1-score gives a single metric balancing precision and recall evaluating the model's performance, especially when the class distribution is imbalanced.

$$\text{Accuracy} = \frac{TP + TN}{TP + TN + FP + FN} \quad (5)$$

$$\text{Precision} = \frac{TP}{TP + FP} \quad (6)$$

$$\text{Recall} = \frac{TP}{TP + FN} \quad (7)$$

$$F1 = \frac{2TP}{2(TP + FP + FN)} \quad (8)$$

We also estimated variable importance using permutation feature importance to explore their contributions to fruit tree classification. This compares the accuracy of the model without a specific variable to the fitted model. The result was evaluated by mean decreased accuracy for each variable. The more important the variable, the higher the decreased accuracy value.

3. Results and discussion

3.1. Spectral and textural information of different fruit trees

The potential to differentiate tropical fruit trees based on spectral bands and textural information derived from Sentinel-2 and Planet images is demonstrated visually in Fig. 4, which visualizes the overlapping rate (OR) between different pairs of fruit trees corresponding to each information band. The overlapping rate estimates an identical shade between two density graphs, constructed from extracted data points to reveal how much these two graphs of a specific index are similar (Pastore, 2018). The higher the overlapping rate, the more difficult it is to distinguish two fruit trees based on that index. The fruit trees in the study area are all tropical fruit trees with relatively similar biophysical characteristics. Therefore, these fruit trees are relatively difficult to discriminate with most overlapping rates above 50 %. Some of them are even identical when considering entire indices, such as coconut versus coconut intercropping (OR = 91.1 %), durian versus rambutan (87.7 %), and durian versus pomelo (86.3 %). It means that isolating other fruit trees from coconut and coconut intercropping gardens is challenging.

In terms of spectral and textural information, they were also grouped into three main groups based on overlapping rates reflecting

Table 3
Hyper-parameters were used in five machine learning models.

Model	Hyper-Parameters
K-Nearest Neighbor (KNN)	n_neighbors = 5
Gradient Boosting Machine (GBM)	n_estimators = 100, learning_rate = 0.1, max_depth = 2
Naive Bayes (NB)	priors = None, var_smoothing = 1e-09
Random Forest (RF)	n_estimators = 200, max_depth = 10, max_features = 'sqrt'
Support Vector Machine (SVM)	kernel = 'rbf', C = 1, degree = 3, gamma = 'scale'

*Note: Other hyper-parameters in the above machine learning models are set as default values.

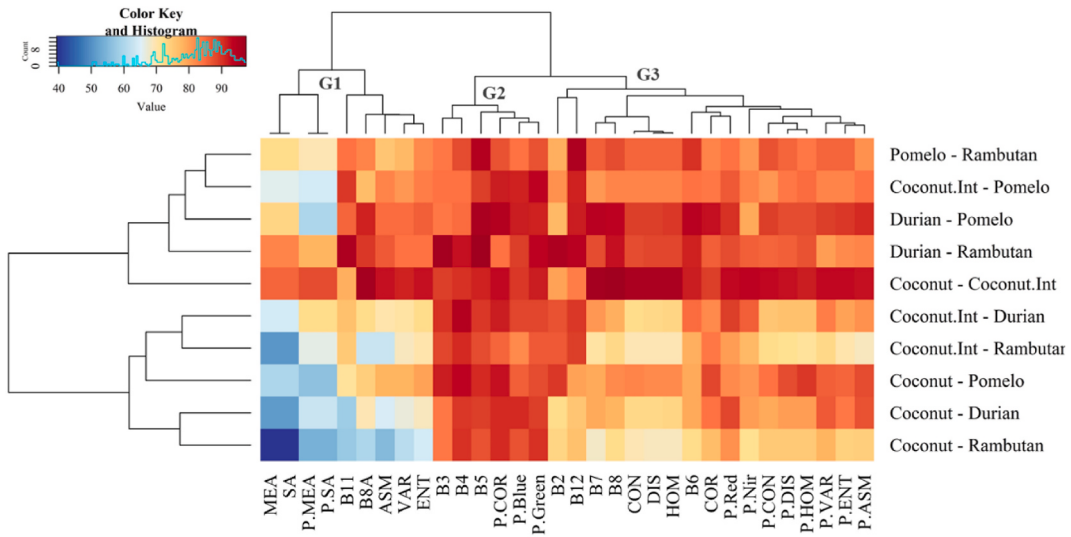


Fig. 4. Heatmap illustrates overlapping rates between different pairs of fruit trees over spectral bands and textural indices. Prefix P. indicates Planet-derived information. Dendograms group fruit tree combination and indices into identical clusters.

discrimination ability among these fruit trees. Group 2 (G2) has a low discrimination ability with an almost overlapping rate above 80 %. Group 3 (G3) shows good discrimination ability for coconut and coconut intercropping from other fruit trees, accounting for about half of the information bands. Group 1 (G1) implies exceptional differentiation for coconut and others with low overlapping rates (OR < 70 %) as well as a promising ability to distinguish the remaining species.

3.2. Classification performance from machine learning and CNN models

The machine learning and CNN models were trained and tested using two separate datasets to investigate the classification capability of fruit trees. Spectral bands and textural indices from both Sentinel-2 and Planet were included in the classification. The general results yielded different overall accuracy and F1-score across classifiers (Fig. 5), overall accuracy and F1 reflect general power of model and performance of multi-classification models. Specifically, NB showed a relatively low classification capability, with accuracy of 40 % and F1-score of 32 %. SVM had a medium classification capability (accuracy and F1-score approximately 61 % and 48 %). A group of two classifiers (including RF and GBM) performed relatively accurate classification, about 70 % accuracy, and F1-score achieved from 63 to 65 %. Among them, KNN and CNN indicated exceptional capability in distinguishing fruit trees with an accuracy of about 88–89 %. The F1 scores for KNN and CNN are fairly comparable, yet CNN is a slightly better classifier based on accuracy and F1-score.

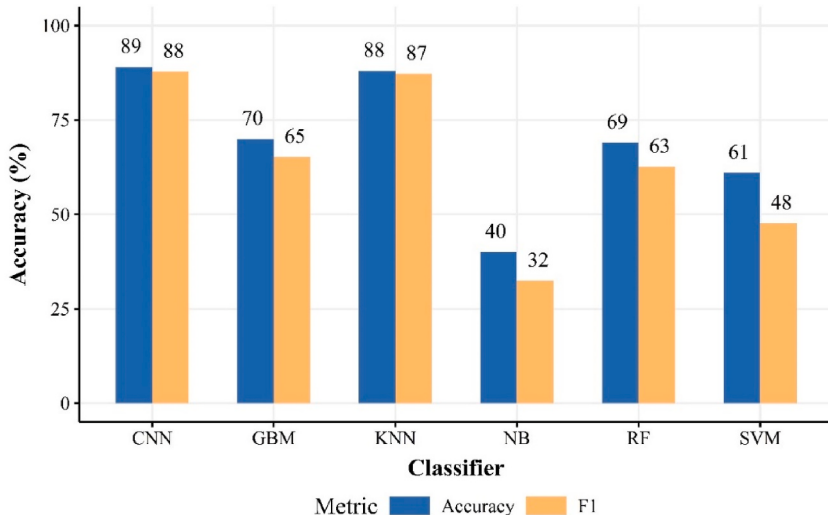
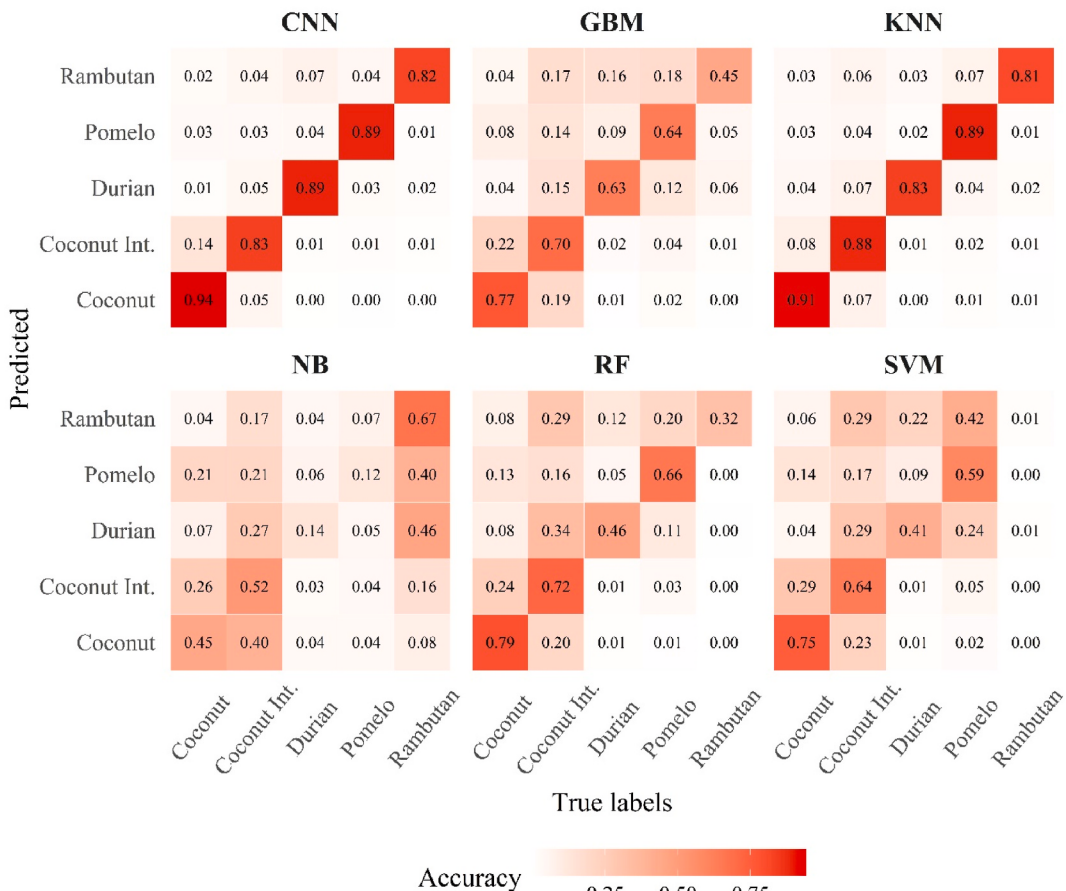


Fig. 5. Overall accuracy and F1-score were obtained from different models in fruit tree classification.

The confusion matrix of six machine learning and CNN models illustrates the performance of classifiers for each individual fruit tree (Fig. 6). CNN and KNN models generally achieved fairly high performance for all fruit trees, as reflected by the above overall accuracy. More explicitly, coconut was best classified by CNN (94 %), followed by KNN, RF, GBM, SVM, and NB in descending order. KNN expressed the highest performance for coconut intercropping (88 %), followed by CNN (83 %). GMB, RF, and SVM showed medium-high capacity, approximately 64–72 %. In contrast, nearly half of coconut intercropping was misclassified by the NB classifier. Major misclassifications were found between coconut intercropping and coconut monocultures, with the highest error rate was up to 26 % (NB). There were only three models that had high performance in durian tree recognition, which were detected by CNN (89 %), KNN (83 %), and GBM (63 %). SVM and RF had a relatively similar performance, which only identified around 41–46 %. The remaining were assigned to coconut intercropping and pomelo trees. Only 14 % of durian trees were accurately classified by NB, while the remaining 46 % were supposed to be rambutan trees. CNN and KNN had an identically high performance for pomelo classification (89 %). The small confusions between pomelo and coconut, coconut intercropping, and durian trees were found in GBM, RF, and SVM, limiting the classification capacity of these classifiers. Therefore, these models were only able to detect pomelo at a medium accuracy, approximately 59–66 %. Although NB often shows low performance, especially for pomelo (only 12 %), it exceptionally detected rambutan trees (67 %). Its capacity in pomelo detection was even higher than that of SVM (1.1 %), RF (32 %), and GBM (45 %). The SVM model could barely recognize rambutan using the current data of spectral and textural information, although it showed relatively high performance for other fruit trees, with 90 % misclassification for coconut intercropping and pomelo trees. Besides, CNN and KNN still lead in terms of performance for rambutan trees, which achieved approximately 81–82 % accuracy.

3.3. Spatial agreement between classified maps and reference layer

Spatial agreement compares classified maps from the trained models (Fig. 7 and Supplementary data) and reference layer, thereby reflecting the reliability of the models on data outside the training data or real data. Overall, spatial agreement increases gradually as follows: NB (39.2 %) < RF (52.2 %) < KNN (53.2 %) < SVM (53.7 %) < GBM (55.6 %) < CNN (56.9 %). This trend aligns with the accuracy assessment, where NB exhibited the lowest performance and CNN the highest. In the previous assessment, KNN had the second-highest accuracy, which was only slightly lower than CNN. Yet, the spatial assessment revealed instability in the classification



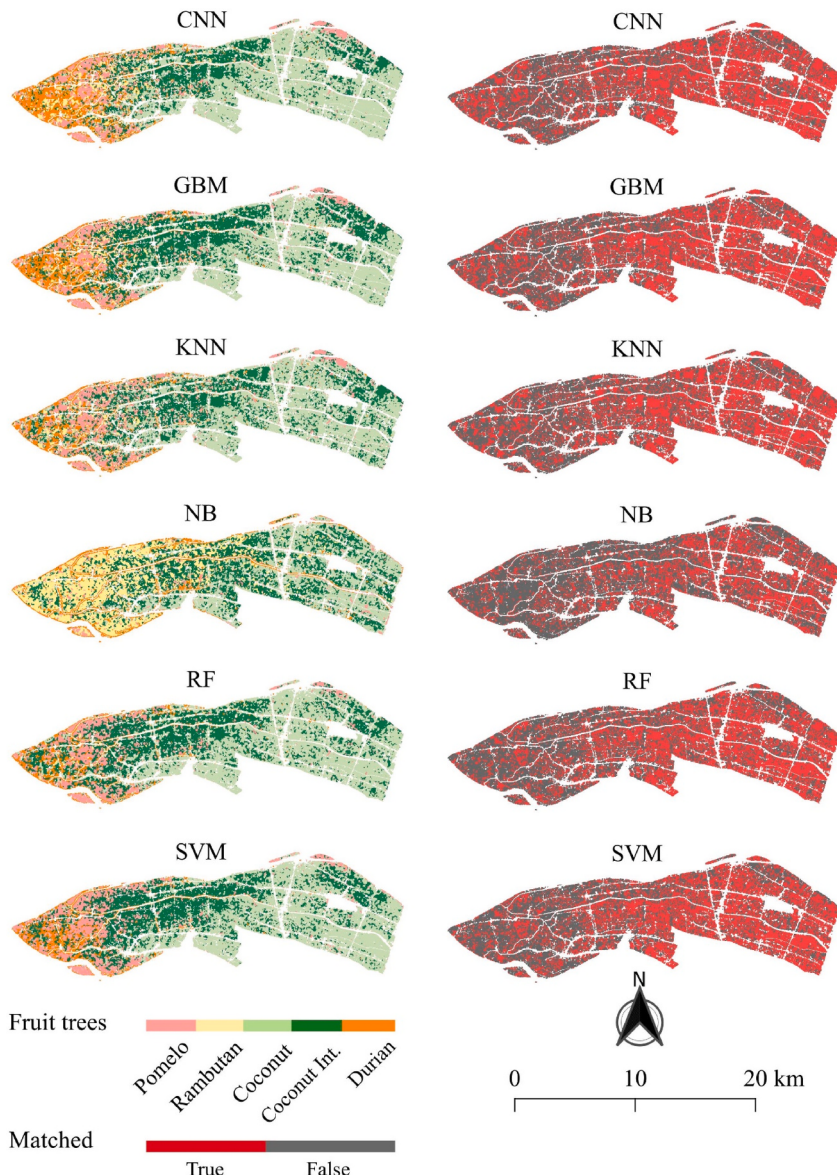


Fig. 7. Fruit tree maps obtained from different machine learning and CNN models based on spectral and textural indices from Sentinel-2 and Planet images (left panel) and spatial agreement between classified maps and reference layer (right panel). True = Matched, False = Unmatched.

of KNN compared to CNN. CNN has a high spatial agreement (higher than 40 %) for every individual category except for rambutan (only 27.8 %), with the highest value belonging to coconut (68.8 %). However, it should be noted that individual spatial agreement of categories may be different between the models. The highest agreement for coconut was found in GBM (approximately 72.1 %). Meanwhile, KNN and RF disclosed the highest spatial agreement for durian and rambutan, respectively. Coconut intercropping, pomelo, and durian are fruit trees with high spatial agreement detected by the CNN model.

3.4. Important variables in fruit tree classification

In the CNN model, one variable is removed from the model to estimate a decrease in accuracy and reflect the importance level of each variable (Fig. 8). It reveals that Band 11 (SWIR1, Sentinel-2) is the most important variable in both the CNN model and individual fruit tree classification. The decreased accuracy level in the CNN model is up to 26.4 %. The other Sentinel-2 spectral bands (i.e., Band 5, Band 2, Band 8A) also contributed around 12–12.6 % to the classification accuracy. Textural indices from Planet (i.e., ENT and ASM) considerably reduced the classification accuracy by 9.7–11.9 %. About 6–7 % of accuracy is constituted by Sentinel-2 spectral bands of Band 4, Band 12, band 6, and Band 7. Besides, a group of textural indices from Planet (e.g., MEA, SA, HOM, COR, and CON) are also important variables in the CNN model to distinguish fruit trees, with decreased accuracy above 5 %.

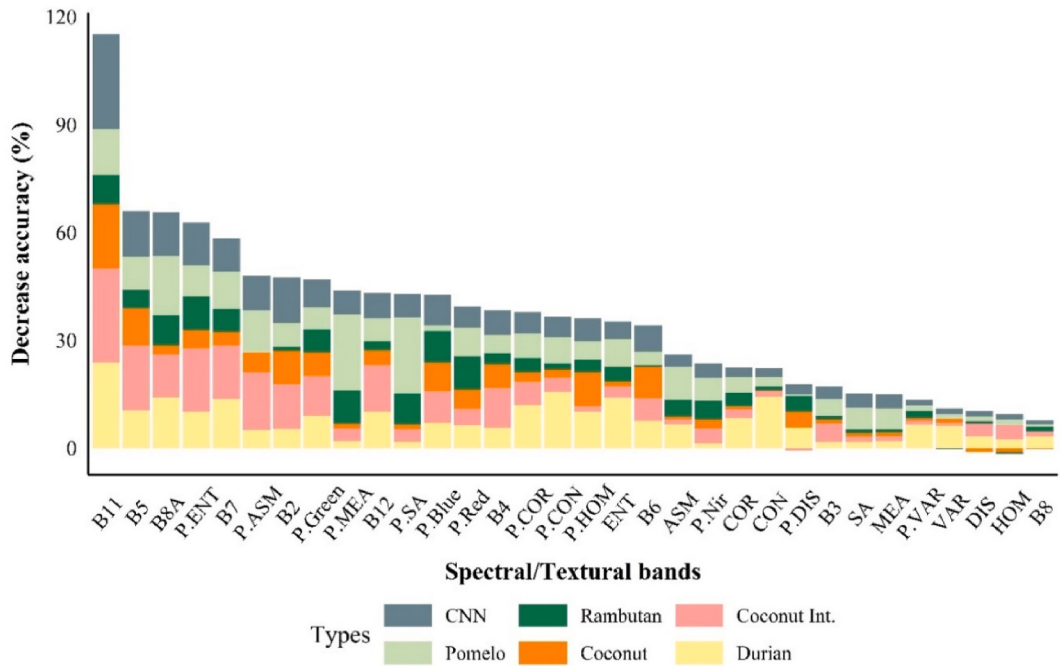


Fig. 8. Variable importance is estimated for the CNN model and each individual fruit trees. Prefix letter “P.” indicates Planet-derived spectral and textural information.

More specifically, the variables assisting in pomelo detection are Planet textural indices of MEA and SA, with a decreased accuracy of approximately 21 % (ASM, 11.7 %). Spectral bands from Sentinel-2 significantly improved their accuracy from 10 % up to 16.6 % (i.e., Band 5, Band 7, Band 11, and Band 8A).

In rambutan recognition, the classification sensitivity is mainly participated by Planet-based indicators, such as textural indices (ENT, MEA, SA) and spectral bands (Red, Blue, and Green bands), with an accuracy of about 6.5–9.3 %. Spectral bands from Sentinel-2, such as Band 8A, Band 11, Band 5, and Band 7, are also critical in the classification.

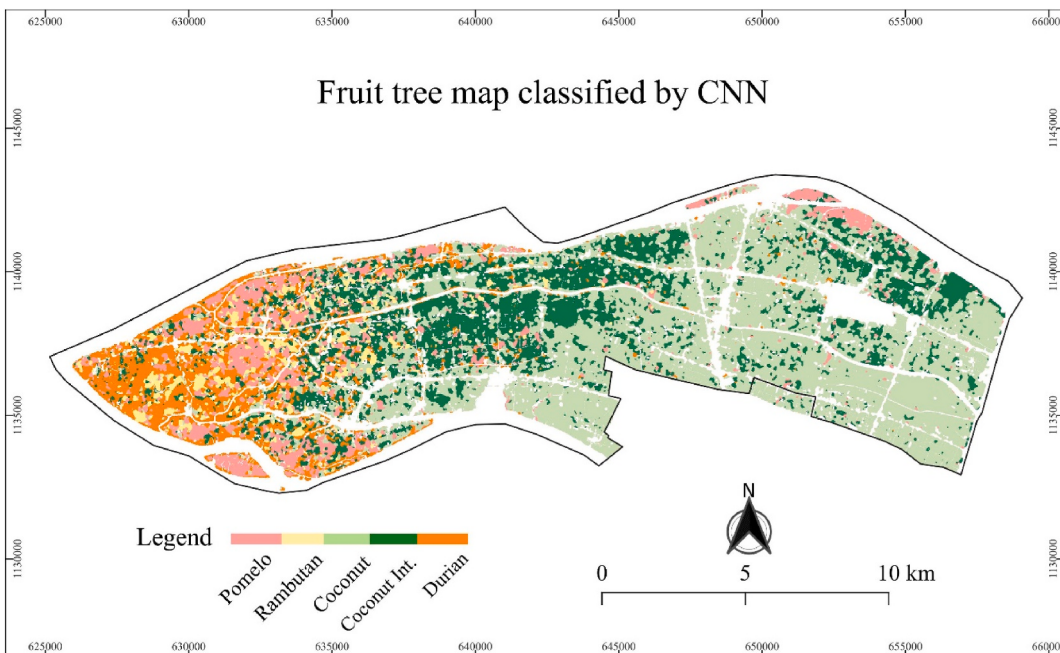


Fig. 9. Classified fruit tree map obtained from CNN model using spectral and textural indices from Sentinel-2 and Planet images.

In contrast, Sentinel-2 spectral bands tend to be more important in the classification of coconut and coconut intercropping. For example, the absence of Band 11 in the classification reduces the classification performance by 26.2 % (coconut intercropping) and 17.9 % (coconut). The other common Sentinel-2 spectral bands for the classification of these two fruit trees are Band 5, Band 2, Band 4, Band 11, Band 7, and Band 6. The Planet textural indices also improve the classification, yet they are mainly from HOM, ASM, and ENT.

Band 11 of Sentinel-2 decreased the accuracy of durian by 23.8 %, and it is the most informative band for this fruit tree detection. Other Sentinel-2 spectral bands make a modest contribution, about 10–14 % (Band 8A, Band 7, Band 5, and Band 12). It is followed by Planet-based CON (15.7 %). It should be noted that durian is effectively distinguished by Sentinel-2 textural indicators, such as CON and ENT (14–14.4 %).

3.5. Mapping fruit trees using CNN model

[Fig. 9](#) depicts the predicted fruit tree map by the CNN model and a combination of spectral bands and textural indices from both Sentinel-2 and Planet images, which is based on the trained model with above accuracy and F1-score performance. This spatial fruit tree map clearly illustrates the spatial distribution of individual fruit trees in the study areas, which was verified through our secondary field surveys and confirmed to have high similarity with actual statistics by local authorities. Yet, there is still a discrepancy in the total area between the statistical area and classified areas. Coconut has the lowest disparity when the classified area is higher than the statistics at about 5.8 %. In contrast, a significant mismatch was found in rambutan, classified as less than the statistical area, about 2,593 ha.

About half of the total fruit growing area in the district is coconut farms (73,038 ha, 49 %), mainly concentrated in a large and uniform area in the east and southeast of the study area. The remaining quarter is coconut intercropping with other crops/fruit trees under the coconut canopy (37,150 ha) in the northeast and central part of the study area, where the junction between monoculture coconut and other fruit trees is considered as a junction and has high potential for conversion. The areas of durian and pomelo account for 11.2 % (16,705 ha) and 10.5 % (15,717 ha), which are mainly distributed in the west or the fertile headland of the islet. The remaining fruit-growing areas (6,468 ha) are rambutan, which is also found in the specialty fruit-growing regions of the headland islet. However, the rambutan gardens are more dispersed than other fruit gardens.

3.6. Discussions

Several efforts have been made to identify fruit species in orchards, mainly for subtropical and temperate families rather than tropical fruits. The previous studies mainly adopted advanced data sources such as UAV, Aerial photos, LIDAR, and very high-resolution images to detect fruit species ([Ozdarici Ok and Ok, 2023b](#)). These advanced technologies can gain more efficiency with scientific rigor. Yet, it is supposed to be challenging to replicate in extensive areas in developing countries because of technical and financial constraints. This study plays as one of a pioneering case studies to leverage the combination of freely accessible satellite data sources, textural features, and modern image analyses from machine learning and deep learning classifiers in the identification of tropical fruit trees. The proposed approach based on spectral and textural indicators from both Sentinel-2 and Planet images yielded a relatively good accuracy (approximately 89 %) with high spatial agreement compared to reference data as well as verified by local departments (Section 3.2 and Section 3.3). It also demonstrates the potential for large-scale replication, as opposed to UAV-based data, which is typically only applicable at the smallholder level.

The current studies mainly exploit temporal signals from time series data to distinguish tree species ([Peña and Brenning, 2015](#); [Zhou et al., 2022b](#)). It only shows high potential for temperate fruit species with clear leaf-shedding and flowering seasons or between species with very different leaf-shedding and flowering seasons. For tropical fruit trees, they are mostly evergreen all year round. Although they have a leaf-growing season, they usually occur simultaneously in the rainy season. Therefore, even using time series images can hardly help in identification (Section 3.1). Also, obtaining continuous time series images in tropical monsoon climate regions is not easy due to the influence of clouds during the rainy season. Meanwhile, their leaf and canopy characteristics are relatively different, for example, pomelo leaves often have broader leaf blades than rambutan leaves, which has the potential to differentiate between them. It was proved via our analysis that textural information reflecting leaves and canopy characteristics always appears among the most important variables for classification (Section 3.4). Planet-based textural indices are more critical than Sentinel-2 textural indices because of their finer spatial resolution, which captures more textural details to discriminate fruit trees. In contrast, Sentinel-2, with its broad spectral range, plays a key role in contributing spectral bands to the classification process, particularly in the infrared and shortwave infrared wavelengths which are essential for assessing vegetation health and conditions.

Among the considered models, CNN showed the highest and fairly balanced performance for different fruit tree classifications (indicated by the confusion matrix, Section 3.2). However, based only on evaluation parameters such as accuracy and F1-score, it is difficult to determine the most appropriate model because KNN also showed promising results. This is really surprising because KNN frequently has lower classification performance than other models. Yet, its predicting capability in an independent dataset for mapping entire areas significantly dropped compared to CNN. This implies that whether a model is suitable or not depends on its performance on the entire spatial map rather than just evaluating solely the evaluation parameters. Instead of applying a single model, users can adopt a specific model for their needs. For example, GBM has a good performance for coconut detection with high spatial agreement, while RF can yield a high spatial agreement for rambutan compared to the CNN model. It can also generate a probability map of fruit distribution by combining different models to leverage their powers instead of a typical single-class map. Our analysis of the variable importance of each fruit type also suggests the potential for application for specific purposes. For instance, when we need to identify

pomelo trees, we only need to extract and input into the model the top information bands that are the most important for classifying pomelo instead of all total 32 variables of spectral and textural layers. It therefore can save time on data preparation and resources for model training and prediction.

This experimental study has been completed with an attempt to leverage both spectral information and textural features from freely accessible high and medium resolution images, utilizing the simplicity of 1D-CNN model to map fruit tree species with a relatively high accuracy. It also provides insightful and fair comparisons across approaches and asserts that CNN overpassed the other conventional methods, even with the simplicity of one-dimensional architecture. It also promises scalability with fully available data sources and transparent methodology. Yet, it still has certain limitations that should be addressed and improved in future work. The deep learning model (CNN) frequently requires extensive training and validating datasets, however, this study even produced acceptable accuracy, and our dataset was still moderate. It requires an expansion of the training data in a two-dimensional format with spatial explicitness to upgrade the current one-dimensional architecture to a two-dimensional network (2D-CNN), which can promisingly improve the current fruit trees map. Since tropical fruit trees often exhibit similar features that lead to misclassification, attention mechanisms should be incorporated into the network architecture to enhance species classification. Furthermore, pilot studies should be conducted in similar regions to validate the model's effectiveness as a basis for large-scale research.

4. Conclusion

The CNN model demonstrated better classification performance for the distribution of fruit trees compared to other machine learning models such as GBM, KNN, NB, RF, and SVM. Spectral bands and textural indices acquired from freely available remote sensing data sources of Sentinel-2 and Planet were leveraged to detect different kinds of tropical fruit species. The CNN model exploited spectral information mainly from Sentinel-2 and textural features from Planet to distinguish between five main fruit species, including coconut, coconut intercropping, durian, pomelo, and rambutan, with a relatively high accuracy (89%). Coconut and coconut intercropping have the highest accuracy and spatial agreement, while rambutan and durian are challenging to discriminate from others. The most significant spectral contributors to the classification are Band 11, Band 2, Band 5, and Band 8A (Sentinel-2). Besides, Planet improves the classification by textural features of ENT, ASM, MEA, SA, HOM, COR, and CON.

The result fruit tree map developed by the CNN model achieved high performance and spatial similarity as well as major distribution zones to local references and statistics. Yet, there is still a mismatch in terms of total growing areas, mostly for rambutan because of small and discrete growing areas.

This research is an effort to classify tropical fruit species totally based on freely accessible datasets of Sentinel-2 and Planet that leverages spectral and textural information instead of costly and highly advanced data sources. It has promising potential for future replication in other tropical areas with similar characteristics. The trained CNN model has been given in the GitHub project repository (https://github.com/canng/RSASE_cnnTropiTrees). However, it should be further developed to improve classification performance, especially for more fruit species.

CRediT authorship contribution statement

Can Trong Nguyen: Writing – review & editing, Visualization, Validation, Methodology, Formal analysis, Conceptualization. **Phan Kieu Diem:** Writing – review & editing, Supervision, Methodology, Conceptualization. **Dang Hieu Nghia:** Visualization, Validation, Formal analysis. **Nguyen Kieu Diem:** Writing – review & editing, Conceptualization. **Nguyen Thi Hong Diep:** Writing – review & editing, Conceptualization. **Thanh-Noi Phan:** Writing – review & editing, Conceptualization. **Vo Quang Minh:** Writing – review & editing, Conceptualization. **Nguyen Hong Quang:** Writing – review & editing, Conceptualization.

Ethical statement

We, the authors, hereby declare that this manuscript is our original work and has not been published or submitted elsewhere for publication. All data, analyses, and interpretations presented in this study have been conducted with integrity and transparency.

We affirm that this research adheres to the ethical guidelines. There are no conflicts of interest that could influence the results or interpretations of this study.

All authors have read and approved the final version of the manuscript and agree to its submission to Remote Sensing Applications: Society and Environment (RSASE).

Declaration of competing interest

The authors declare that they have no known competing financial interests or personal relationships that could have appeared to influence the work reported in this paper.

Acknowledgement

The authors would like to sincerely thank the project "Assessment of Land Resources for Sustainable Agricultural Development in Chau Thanh District, Ben Tre Province" (TDH2021-06), funded by Can Tho University, for providing valuable field data, which significantly contributed to the data analysis and completion of this article. We also respectfully dedicate this work to commemorate our co-author

Dang Hieu Nghia, whose passing is a profound loss to our team, leaving his invaluable contributions unfinished.

Appendix A. Supplementary data

Supplementary data to this article can be found online at <https://doi.org/10.1016/j.rsase.2025.101633>.

Data availability

The trained CNN model has been given in the GitHub project repository (https://github.com/canng/RSASE_cnnTropiTrees)

References

- Alzhanov, A., Nugumanova, A., 2024. Crop classification using UAV multispectral images with gray-level co-occurrence matrix features. *Procedia Comput. Sci.* 231, 734–739. <https://doi.org/10.1016/j.procs.2023.12.145>.
- Ba, N.T.B., Nhung, V.T.N., 2013. Potentials and development orientation of tourism in Chau Thanh district, Ben Tre province. *J. Sci. Ho Chi Minh Univ. Educ.* 49, 180–186. [https://doi.org/10.54607/hcmue.js.0.49.1929\(2013](https://doi.org/10.54607/hcmue.js.0.49.1929(2013).
- Bhosale, K., Musande, V., 2019. Evaluation of deep learning CNN model for land use land cover classification and crop identification using hyperspectral remote sensing images. *J. Indian Soc. Remote Sens.* 47, 1949–1958. <https://doi.org/10.1007/s12524-019-01041-2>.
- Can, T.N., Chidhaisong, A., Diem, P.K., Huo, L.Z., 2021. A modified bare soil index to identify bare land features during agricultural fallow-period in southeast asia using landsat 8. *Land* 10, 1–18. <https://doi.org/10.3390/land10030231>.
- Dalagnol, R., Wagner, F.H., Galvão, L.S., Braga, D., Osborn, F., Sagang, L.B., da Conceição Bispo, P., Payne, M., Silva Junior, C., Favrichon, S., Silgueiro, V., Anderson, L.O., Aragão, L.E.O. e. C. de, Fenholz, R., Brandt, M., Ciais, P., Saatchi, S., 2023. Mapping tropical forest degradation with deep learning and Planet NICFI data. *Remote Sens. Environ.* 298. <https://doi.org/10.1016/j.rse.2023.113798>.
- Deng, X., Zhu, Z., Yang, J., Zheng, Z., Huang, Z., Yin, X., Wei, S., Lan, Y., 2020. Detection of citrus huanglongbing based on multi-input neural network model of UAV hyperspectral remote sensing. *Remote Sens.* 12, 1–20. <https://doi.org/10.3390/RS12172678>.
- Dong, X., Zhang, Z., Yu, R., Tian, Q., Zhu, X., 2020. Extraction of information about individual trees from high-spatial-resolution uav-acquired images of an orchard. *Remote Sens.* 12, 1–21. <https://doi.org/10.3390/RS12010133>.
- Ferreira, M.P., Zortea, M., Zanotta, D.C., Shimabukuro, Y.E., de Souza Filho, C.R., 2016. Mapping tree species in tropical seasonal semi-deciduous forests with hyperspectral and multispectral data. *Remote Sens. Environ.* 179, 66–78. <https://doi.org/10.1016/j.rse.2016.03.021>.
- Georgosan, S., Grippa, T., Vanhuyse, S., Lenner, M., Shimoni, M., Wolff, E., 2018. Very high resolution object-based land use-land cover urban classification using extreme gradient boosting. *Geosci. Rem. Sens. Lett. IEEE* 15, 607–611. <https://doi.org/10.1109/LGRS.2018.2803259>.
- Hall-Beyer, M., 2017. *GLCM Texture: A Tutorial V. 3.0. Canada, Alberta*.
- Hanh, H.Q., Azadi, H., Dogot, T., Ton, V.D., Lebailly, P., 2017. Dynamics of agrarian systems and land use change in North Vietnam. *Land Degrad. Dev.* 28, 799–810. <https://doi.org/10.1002/ldr.2609>.
- Iqbal, N., Mumtaz, R., Shafii, U., Zaidi, S.M.H., 2021. Gray level co-occurrence matrix (GLCM) texture based crop classification using low altitude remote sensing platforms. *PeerJ Comput. Sci.* 7, 1–26. <https://doi.org/10.7717/PEERJ-CS.536>.
- Jodzani, S.E., Johnson, B.A., Chen, D., 2019. Comparing deep neural networks, ensemble classifiers, and support vector machine algorithms. *Remote Sens.* 11, 1–24.
- Kabir, S., He, D.C., Sanusi, M.A., Wan Hussina, W.M.A., 2010. Texture analysis of IKONOS satellite imagery for urban land use and land cover classification. *Imag. Sci. J.* 58, 163–170. <https://doi.org/10.1179/136821909X12581187860130>.
- Kumar, S., Singh, P., Sikka, G., 2022. A deep learning approach to intelligent fruit identification and family classification. *Multimed. Tool. Appl.* 81 (17), 24379–24398. <https://doi.org/10.1007/s11042-022-12942-9>.
- Kupidura, P., 2019. The comparison of different methods of texture analysis for their efficacy for land use classification in satellite imagery. *Remote Sens.* 11. <https://doi.org/10.3390/rs11101233>.
- Liu, Y., Xue, Y., Zhou, L., Zhang, H., 2017. Image-based fruit category classification by 13-layer deep convolutional neural network and data augmentation. *Multimed. Tool. Appl.* 77 (22), 29669–29683. <https://doi.org/10.1007/s11042-017-5243-3>.
- Mohammadpour, P., Viegas, D.X., Viegas, C., 2022. Vegetation mapping with random forest using Sentinel 2 and GLCM texture feature—a case study for lousã region, Portugal. *Remote Sens.* 14. <https://doi.org/10.3390/rs14184585>.
- Mureşan, H., Oltean, M., 2021. Classification of plants by their fruits and leaves using convolutional neural networks. *J. Plant Res.* 134 (4), 923–935. <https://doi.org/10.1007/s10265-021-01352-6>.
- Nery, T., Sadler, R., Solis-Aulestia, M., White, B., Polyakov, M., Chalak, M., 2016. Comparing supervised algorithms in land use and land cover classification of a landsat time-series. *Int. Geosci. Remote Sens. Symp.* 5165–5168. <https://doi.org/10.1109/IGARSS.2016.7730346>.
- Nguyen, C.T., Chidhaisong, A., Limsakul, A., Varnakovid, P., Ekkawatpanit, C., Diem, P.K., Diep, N.T.H., 2022. How do disparate urbanization and climate change imprint on urban thermal variations? A comparison between two dynamic cities in Southeast Asia. *Sustain. Cities Soc.* 82. <https://doi.org/10.1016/j.jscs.2022.103882>.
- Nguyen, C.T., Kaewthongrach, R., Channumsin, S., Chongcheawchamnan, M., Phan, T.N., Niammud, D., 2023. A regional assessment of ecological environment quality in Thailand special economic zone: spatial heterogeneous influences and future prediction. *Land Degrad. Dev.* <https://doi.org/10.1002/ldr.4876>.
- Noi, P.T., Kappas, M., 2018. Comparison of random forest, k-nearest neighbor, and support vector machine classifiers for land cover classification using sentinel-2 imagery. *Sensors* 18. <https://doi.org/10.3390/s18010018>.
- Ozdarici Ok, A., Ok, A.O., 2023a. Using remote sensing to identify individual tree species in orchards: a review. *Sci. Hortic. (Amsterdam)* 321, 112333. <https://doi.org/10.1016/j.scientia.2023.112333>.
- Ozdarici Ok, A., Ok, A.O., 2023b. Using remote sensing to identify individual tree species in orchards: a review. *Sci. Hortic. (Amsterdam)* 321, 112333. <https://doi.org/10.1016/j.scientia.2023.112333>.
- Pal, M., 2005. Random forest classifier for remote sensing classification. *Int. J. Rem. Sens.* 26, 217–222. <https://doi.org/10.1080/01431160412331269698>.
- Palanisamy, P.A., Jain, K., Bonafoni, S., 2023. Machine learning classifier evaluation for different input combinations: a case study with landsat 9 and sentinel-2 data. *Remote Sens.* 15. <https://doi.org/10.3390/rs15133241>.
- Pandey, P., Kington, J., Kanwar, A., Simmon, R., Abraham, L., 2023. Planet basemaps for NICFI data program - addendum to basemaps products specification. Norwegian Ministry of Climate Change. https://assets.planet.com/docs/NICFI_Basemap_Spec_Addendum.pdf.
- Park, Y., Guldmann, J.M., 2020. Measuring continuous landscape patterns with Gray-Level Co-Occurrence Matrix (GLCM) indices: an alternative to patch metrics? *Ecol. Indic.* 109, 105802. <https://doi.org/10.1016/j.ecolind.2019.105802>.
- Park, B.E., Jang, W.S., Yoo, S.K., 2016. Texture analysis of supraspinatus ultrasound image for computer aided diagnostic system. *Healthc. Inform. Res.* 22, 299–304. <https://doi.org/10.4258/hir.2016.22.4.299>.
- Pastore, M., 2018. Overlapping: a R package for estimating overlapping in empirical distributions. *J. Open Source Softw.* 3, 1023. <https://doi.org/10.21105/joss.01023>.

- Pem, D., Jeewon, R., 2015. Fruit and vegetable intake: benefits and progress of nutrition education interventions-narrative review article. *Iran. J. Public Health* 44, 1309–1321.
- Peña, M.A., Brenning, A., 2015. Assessing fruit-tree crop classification from Landsat-8 time series for the Maipo Valley, Chile. *Remote Sens. Environ.* 171, 234–244. <https://doi.org/10.1016/j.rse.2015.10.029>.
- Peña, M.A., Liao, R., Brenning, A., 2017. Using spectrotemporal indices to improve the fruit-tree crop classification accuracy. *ISPRS J. Photogrammetry Remote Sens.* 128, 158–169. <https://doi.org/10.1016/j.isprsjprs.2017.03.019>.
- Pereira Martins-Neto, R., García Tommaselli, A.M., Imai, N.N., Honkavaara, E., Miltiadou, M., Saito Moriya, E.A., David, H.C., 2023. Tree species classification in a complex Brazilian tropical forest using hyperspectral and LiDAR data. *Forests* 14, 1–32. <https://doi.org/10.3390/f14050945>.
- Phiri, D., Simwanda, M., Salekin, S., Ryirenda, V.R., Murayama, Y., Ranagalage, M., Oktaviani, N., Kusuma, H.A., Zhang, T., Si, J., Liu, C., Chen, W.H., Liu, H., Liu, G., Cavur, M., Duzgun, H.S., Kemec, S., Demirkiran, D.C., Chairet, R., Ben Salem, Y., Aoun, M., Kiala, Z., Mutanga, O., Odindi, J., Peerbhoy, K., 2020. Sentinel-2 data for land cover/use mapping: a review. *Remote Sens.* 12, 1–35. <https://doi.org/10.3390/rs12142291>.
- Prasad, P., Loveson, V.J., Chandra, P., Kotha, M., 2022. Evaluation and comparison of the earth observing sensors in land cover/land use studies using machine learning algorithms. *Ecol. Inform.* 68, 101522. <https://doi.org/10.1016/j.ecoinf.2021.101522>.
- Rahaman, M.M., Chen, D., Gillani, Z., et al., 2018. Fruit detection and recognition based on deep learning for automatic harvesting: an overview and review. *Agronomy* 13 (6), 1625. <https://doi.org/10.3390/agronomy13061625>.
- Sameen, M.I., Pradhan, B., Aziz, O.S., 2018. Classification of very high resolution aerial photos using spectral-spatial and convolutional neural networks. *J. Sens.* 1, 7195432. <https://doi.org/10.1155/2018/7195432>.
- Segarra, J., Buchaillot, M.L., Araus, J.L., Kefauver, S.C., 2020. Remote sensing for precision agriculture: Sentinel-2 improved features and applications. *Agronomy* 10, 1–18. <https://doi.org/10.3390/agronomy10050641>.
- Slavin, J.U. of M., Lloyd Beate, P.N.G.R., 2012. Health benefits of fruits and vegetables. *Adv. Nutr.* 3, 506–516. <https://doi.org/10.3945/an.112.002154.506>.
- Sothe, C., Dalponte, M., de Almeida, C.M., Schimalski, M.B., Lima, C.L., Liesenberg, V., Miyoshi, G.T., Tommaselli, A.M.G., 2019. Tree species classification in a highly diverse subtropical forest integrating UAV-based photogrammetric point cloud and hyperspectral data. *Remote Sens.* 11. <https://doi.org/10.3390/rs11111338>.
- Thu, T.A., Chan, V.H., Guong, V.T., 2013. Some selected soil properties of coconut - cocoa intercropping in Chau Thanh - ben Tre. *Can Tho Univ. J. Sci.* 25, 260–270.
- Thuong, V.T., Ha, C.V., 2013. Effectiveness evaluation of agricultural land and proposing land use type for commodity oriented at lucngan district, bac giang province. *J. Sci. Dev.* 11, 542–548.
- Tian, H., Fang, X., Lan, Y., Ma, C., Huang, H., Lu, X., Zhao, D., Liu, H., Zhang, Y., 2022. Extraction of citrus trees from UAV remote sensing imagery using YOLOv5s and coordinate transformation. *Remote Sens.* 14, 1–21. <https://doi.org/10.3390/rs14174208>.
- Tikuye, B.G., Rusnak, M., Manjunatha, B.R., Jose, J., 2023. Land use and land cover change detection using the random forest approach: the case of the upper Blue nile river basin, Ethiopia. *Glob. Challenges* 7, 1–11. <https://doi.org/10.1002/gch2.202300155>.
- Upadhyay, P., Uniyal, D., Bisht, M.P.S., 2019. Hyperspectral remote sensing for temperate horticulture fruit crops in northern-western Himalayan region: a review. *Int. Arch. Photogramm. Remote Sens. Spat. Inf. Sci. - ISPRS Arch.* 42, 333–338. <https://doi.org/10.5194/isprs-archives-XLII-3-W6-333-2019>.
- Vrdoljak, L., Kilić Pamuković, J., 2022. Assessment of atmospheric correction processors and spectral bands for satellite-derived bathymetry using sentinel-2 data in the middle adriatic. *Hydrology* 9. <https://doi.org/10.3390/hydrology9120215>.
- Wang, F., He, Q., Han, F., Zhang, H., Zhao, Q., Sha, X., 2023. Ecological function service value and quantity of fruit-tree economic forests in the semi-arid loess hilly and gully region of central gansu—a case study of the hulu river basin. *J. Resour. Ecol.* 14, 903–913. <https://doi.org/10.5814/j.issn.1674-764x.2023.05.002>.
- Xia, C., Liu, Z., Suo, X., Cao, S., 2020. Quantifying the net benefit of land use of fruit trees in China. *Land Use Policy* 90, 104276. <https://doi.org/10.1016/j.landusepol.2019.104276>.
- Yang, Biyun, Xu, Yong, 2021. Applications of deep-learning approaches in horticultural research: a review. *Horticulture Research* 8 (123), 1–15. <https://doi.org/10.1038/s41438-021-00560-9>.
- Zhang, C., Huang, C., Li, H., Liu, Q., Li, J., Bridhikitti, A., Liu, G., 2020. Effect of textural features in remote sensed data on rubber plantation extraction at different levels of spatial resolution. *Forests* 11. <https://doi.org/10.3390/F11040399>.
- Zhang, Y., Wang, X., Li, X., Du, Y., Atkinson, P.M., 2023. Monitoring monthly tropical humid forest disturbances with planet NICFI images in Cameroon. *Agric. For. Meteorol.* 341, 109676. <https://doi.org/10.1016/j.agrformet.2023.109676>.
- Zhou, X.X., Li, Y.Y., Luo, Y.K., Sun, Y.W., Su, Y.J., Tan, C.W., Liu, Y.J., 2022a. Research on remote sensing classification of fruit trees based on Sentinel-2 multi-temporal imagers. *Sci. Rep.* 12, 1–14. <https://doi.org/10.1038/s41598-022-15414-0>.
- Zhou, X.X., Li, Y.Y., Luo, Y.K., Sun, Y.W., Su, Y.J., Tan, C.W., Liu, Y.J., 2022b. Research on remote sensing classification of fruit trees based on Sentinel-2 multi-temporal imagers. *Sci. Rep.* 12, 1–14. <https://doi.org/10.1038/s41598-022-15414-0>.